# We are IntechOpen,
# the world's leading publisher of
# Open Access books
# Built by scientists, for scientists

**6,900**
Open access books available

**185,000**
International authors and editors

**200M**
Downloads

Our authors are among the

**154**
Countries delivered to

**TOP 1%**
most cited scientists

**12.2%**
Contributors from top 500 universities

BOOK CITATION INDEX
CLARIVATE ANALYTICS
INDEXED

**WEB OF SCIENCE**™

Selection of our books indexed in the Book Citation Index
in Web of Science™ Core Collection (BKCI)

# Interested in publishing with us?
# Contact book.department@intechopen.com

Numbers displayed above are based on latest data collected.
For more information visit www.intechopen.com

# Regenerative Repair of Bone Defects with Osteoinductive Hydroxyapatite Fabricated to Match the Defect and Implanted with CAD, CAM, and Computer-Assisted Surgery Systems

Koichi Yano, Takashi Namikawa, Takuya Uemura, Yasunori Kaneshiro and Kunio Takaoka

Additional information is available at the end of the chapter

## Abstract

Regenerative repair of large bone defects currently remains a challenging issue during surgery, owing to the limited regenerative ability of the bone. To address this issue, we attempted a precise repair of a bone defect using computer-aided procedures. Using pelvic computed tomography (CT) images of beagle dogs, virtual tumors were created in the pelvis using computer-aided design (CAD), and a bone resection following the margins of the bone tumor was performed on the CAD image. Hydroxyapatite (HA) implants to fill the bone defects and implants for shape evaluation of bone resection sites were designed and produced by computer-aided manufacturing and three-dimensional printing. Subsequently, using a computer navigation system, iliac bone defects were created in beagle dogs as preoperatively planned on CAD, filled with HA implants shaped to fit the bone defect sites, and coated with a recombinant human bone morphogenetic protein (rhBMP)-2-containing dough bone-forming material. Postoperative CT revealed that the new bone was formed around the implant over time. Anatomical healthy bone repair was confirmed to be completed 12 weeks after the surgery. These results demonstrate potential novel technology for efficacious and accurate repair of large bone defects without bone grafting.

**Keywords:** regenerative repair, bone defect, computer-aided design, computer-assisted surgery, 3D printing

## 1. Introduction

Extensive bone defects can occur after severe trauma, infection, or bone tumor resection, and in some cases require bone tissue reconstruction. Therefore, auto/allografts and artificial materials are implanted. Materials currently used for bone tissue reconstruction include autologous bone tissue, such as the ilium and fibula, and allogeneic materials, such as cryopreserved bone, titanium alloys, and bioactive ceramics [1]. Each of these has distinct advantages, but they also have various disadvantages or problems that remain to be solved.

The autologous bone is the most effective material for small bone defects and is characterized by strong bone-forming ability, accompanied by the capability of bone union and remodeling capacity. However, it has disadvantages, including limitations in the collectable quantity and complications after collection, such as pain, infection, fracture, deformation, and risk of damage to major nerves or blood vessels. The use of allogeneic bone is associated with low bone-forming ability; potential transmission of infectious agents; and cost problems, including cleanliness management. Disadvantages of the heterologous bone include possible transmission of animal infections and immunological rejection in addition to those listed for allogeneic bone [2–4].

Although artificial materials offer the advantages of easy access and processing, they are usually incapable of practical bone formation and thus are ineffective for bone regeneration in large bone defects. It is difficult to reconstruct relatively large bone defects in a shape that is anatomically similar to the normal structure.

Scaffolds, growth factors, and cells represent three key elements in regenerative medicine. An ideal approach for bone repair with regenerative medicine technology should have the abilities of osteogenesis, osteoconduction, osteoinduction, and osteointegration to resolve the disadvantages of currently available graft materials. Biocompatible and biodegradable scaffolds include those made of biological materials, such as type 1 collagen and demineralized bone, and of synthetic (artificial) materials, such as porous metals, bioactive glass, synthetic polymers, and calcium phosphate ceramics [hydroxyapatite (HA) and tricalcium phosphate (TCP)] [5].

Among bone morphogenetic proteins (BMP), recombinant human BMP (rhBMP)-2 and -7 are potent osteoinductive cytokines and are clinically used as graft materials in spinal fusion, pseudarthrosis after long bone fractures, repeated posterolateral fusion, and treatment of open fractures of the tibia in some countries, such as European countries and the United States. We expect that they will find increasing application in bone-regenerating medicine because of their high rates of bone union and their simplicity and minimal invasiveness (i.e., bone harvesting is not required) [6–8].

Recent advances in computer-assisted techniques have led to computer-assisted preoperative planning, custom production of surgical implants using patient data, and use of navigation systems in orthopedics. Examples include three-dimensional (3D) printing-based preoperative planning, in which 3D printing of the relevant bone is performed before a trauma patient undergoes surgery and plates to be used are templated with the reference to the simulated

bone so that no intraoperative plate bending maneuvers are required. Furthermore, the pre-bent plate itself serves as a reduction indicator, and accurate corrective osteotomy procedures for malunited fractures are prepared for each patient using osteotomy guides [9, 10]. In addition, the use of navigation systems has been reported to be useful in joint surgery, for example, for accurate installation of artificial joint components, safe and accurate insertion of pedicle screws in spinal fusion, and resection of musculoskeletal tumors [11–13].

These computer-assisted imaging technologies might be applicable for repair of large bone defects that result from wide resection of malignant musculoskeletal tumors. In those cases, the decision regarding optimal resection margins should be based on 3D computed tomography (CT) or/and magnetic resonance imaging (MRI) data to avoid exposure of the tumor tissue to the surgical field and late local recurrence of the tumor, and the image data would be applicable to surgical procedures using computer-assisted navigation surgery (CAS) system. Image data of the virtual bone defect in the computer-aided design (CAD) would be used to fabricate a porous HA block implant with computer-assisted manufacturing system (CAM) to fill the bone defect. To add osteoinductive capacity to the HA implant to accelerate bone defect repair, a cytokine rhBMP-2 with potent osteoinductive capacity retained in its dough-like delivery system is pasted on the HA surface during implantation.

In this study, we investigated the feasibility of computer-assisted technology (CAD, CAM, and CAS) for preoperative surgical planning and corrective surgical procedures to resect a virtual tumor and fabricate an HA implant. Another aim was to estimate the efficacy of rhBMP-2 and its delivery system to promote repair of a large bone defect without bone grafting in a beagle model.

## 2. Experiments

### 2.1. Methods

#### 2.1.1. Preoperative planning

In beagle dogs (male, 10-month-old, body weight: 9–11 kg) scheduled for surgery, pelvic CTs were performed a few days before the surgery, and the acquired data [digital imaging and communication in medicine (DICOM)] were used for preoperative planning with CAD software (Mimics, Magics, Materialise, NV, USA). 3D images created from CT data after DICOM data are transferred to CAD and converted into a standard triangulated language format that can be separated or combined in any way with CAD. On the 3D images of the pelvis obtained in this manner, a virtual bone tumor of 15 mm in diameter was created in the left iliac wing, and a bone resection model was created by establishing the bone resection line, 10 mm distant from the tumor (**Figure 1a** and **b**). An implant was designed to compensate for the defect occurring after resection by subtracting the bone defect part from a mirror image of the right ilium (**Figure 2a**).
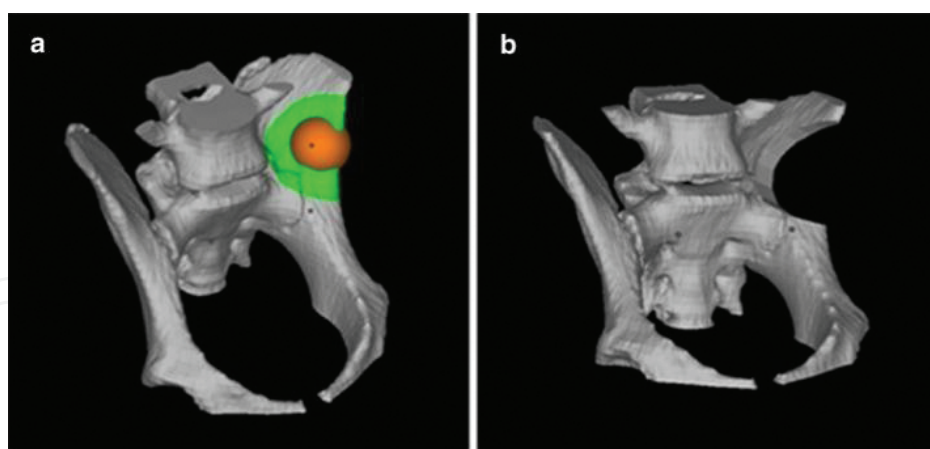
**Figure 1.** (a) A virtual spherical bone tumor of 15 mm in diameter (color: orange) was created in the left iliac wing of the canine pelvis with preoperative planning on computer-aided design (CAD) software. The bone resection line was set 10 mm distant from the bone tumor on the CAD image (color: green). (b) A bone resection model was established on CAD image.
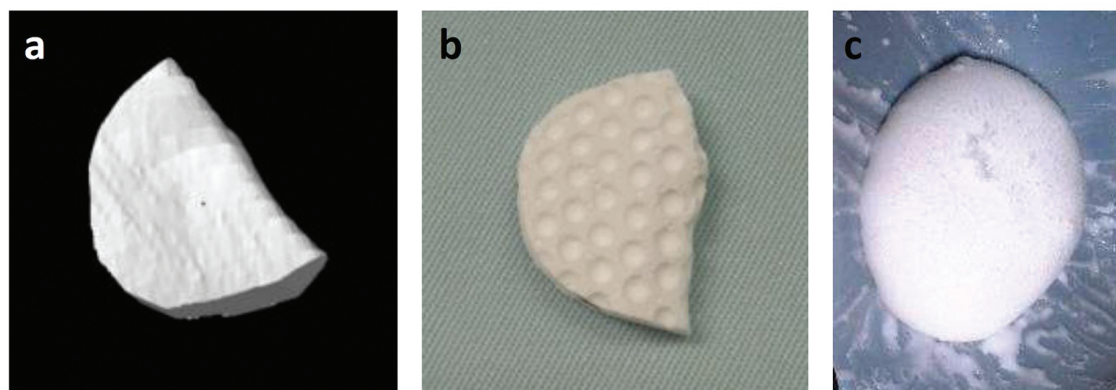


**Figure 2.** (a) CAD image of defected bone generated by subtracting the left iliac bone from the mirror image of the right iliac bone. (b) Fabricated interconnected porous calcium hydroxyapatite (IP-CHA) block by using a 3D drilling machine based on CAD data. Multiple dimples were made to facilitate retention of the BMP-retaining dough material. (c) BMP-retaining biodegradable dough material.

### 2.1.2. Implant preparation

We selected an artificial bone made of interconnected porous calcium HA (IP-CHA, pore size: 150 μm, porosity: 72–78%, MMT Co., Ltd., Osaka, Japan) as a material to fill the defect because of its high osteoconductive capacity [14]. CT data of the bone defect as described above were transferred to a 3D cutting machine (CAM; Modela player, Roland DG Co., Shizuoka, Japan), and an IP-CHA block (cuboid, 40 × 20 × 10 mm) was processed with a 3D drilling machine (MDZ-20, Roland DG Co.). The processed HA block was then machined with a high-speed surgical drill to create a large number of dimples facilitating the application of a BMP-containing dough bone-forming material (described below) (**Figure 2b**). To confirm the size

of the defect at the bone resection site during surgery, CAD design data were migrated to a 3D printer (ZPrinter Z-310, Toyotsu machinery, Aichi, Japan) and printed with gypsum. These were autoclaved or gas sterilized so that they could be used during surgery.

### 2.1.3. Dough bone-forming material

Because BMP administered alone rapidly diffuses in vivo, it cannot maintain the local concentration at a level required for bone formation and thus does not induce bone formation. Therefore, an appropriate slow-release carrier (drug delivery system, DDS) is necessary to accomplish effective bone formation with BMP. Bovine type 1 collagen is currently used as a DDS for BMP, but it has the disadvantages of requiring a large amount of expensive BMP and the potential transmission of pathogens, such as variant Creutzfeldt-Jakob disease, which cannot be completely excluded [4].

To solve these problems, our group has developed a poly-d, l-lactic acid-polyethylene glycol block copolymer (PLA-PEG, Taki Chemical Co., Ltd., Kakogawa, Japan), which is a fully synthetic artificial DDS material that reduces the BMP dose required for bone formation [15–25]. Given that the PLA-PEG polymer is viscous at room temperature, it is difficult to process manually but can be transformed into a dough-like material by the addition of powdery β-TCP, which can be readily processed. By adding BMP to this mixture, we devised a dough-like bone-forming material (**Figure 2c**) [26–32]. rhBMP-2 was synthesized by *Escherichia coli* transfected with the rhBMP-2 gene. After inactive monomer rhBMP-2 molecules were produced, they were dimerized to active rhBMP-2 by biochemical processing. The BMP-2 delivery system for one IP-CHA implant was generated by mixing 100 μg of rhBMP-2 (Osteopharma Inc., Osaka, Japan), 200 mg of powdery β-TCP (particle size <100 μm in diameter, Olympus Biomaterial Corp., Tokyo, Japan), and 200 mg of the PLA-PEG polymer [33]. Physiochemical characteristics of this dough bone-forming material have been reported previously. Dough bone-forming material preparations devoid of rhBMP-2 were prepared as the control group. The samples were stored at −30°C until use during surgery.

### 2.2. Bone resection with the navigation system and implantation of BMP-added IP-CHA implant

Data of the bone resection model created with CAD software were converted into the DICOM format. Converted DICOM data were transferred to a CT-based computer navigation system (Stealth Station Tria, Medtronic Navigation, Louisville, Co, USA). Anesthesia, ketamine (10 mg/kg) and xylazine (1.2 mg/kg) was injected intramuscularly and maintained with a continuous pentobarbital (25 mg/kg) intravenously. The left ilium was opened at the acetabular margin in beagle dogs in the right lateral decubitus position. A reference frame was secured to the iliac wing with two threaded pins and matched with navigation by point and surface registration. A Surgairtome equipped with a passive pointer was used for bone resection. Bone resection was performed as preoperatively planned according to the navigation system. The accuracy of bone resection was evaluated by testing the fit of the 3D printer-produced gypsum implant. The dough bone-forming material was then pasted evenly on the surface of the preoperatively designed and processed HA implant, and the coated implant was secured with

two or three 0.6 mm wires (Synthes Co., Ltd., Tokyo, Japan). The implant was carefully sutured in place to ensure contact with the surrounding muscle. A prophylactic antibiotic agent (10 mg/kg body weight) was administered to animals before and after the surgery. This animal experiment was performed after institutional approval was obtained.

### 2.3. Evaluation of efficacy of computer-assisted bone defect repairing system

CT slice images of the iliac bone were obtained immediately and 3, 6, 9, and 12 weeks post-operatively to observe the bone repair reaction at the bone defect site and reconstructed into slice and 3D images as desired using the reconstruction software (Aze, Tokyo, Japan). CT images of the mid-axial slice of the implant and the next slice 1 mm from the center were analyzed. A high-density area surrounding the implant was considered to be a new bone area and quantified with ImageJ software (Wayne Rasband, National Institutes of Health, Bethesda, MD). Results were statistically analyzed by the Mann-Whitney U test with a significance level of $P < 0.05$. The ilium was harvested 12 weeks postoperatively and fixed in 70% ethanol. From un-decalcified specimens, 10 μm sections were prepared and subjected to Villanueva bone staining for histological evaluation. Specimens were macroscopically evaluated.

## 3. Results

### 3.1. Accuracy of iliac bone resection by computer-aided surgery

In all animals, navigation-guided osteotomy could be accurately performed on the virtual bone tumor exactly as planned on the CAD system. The CAD-designed, 3D printer-produced
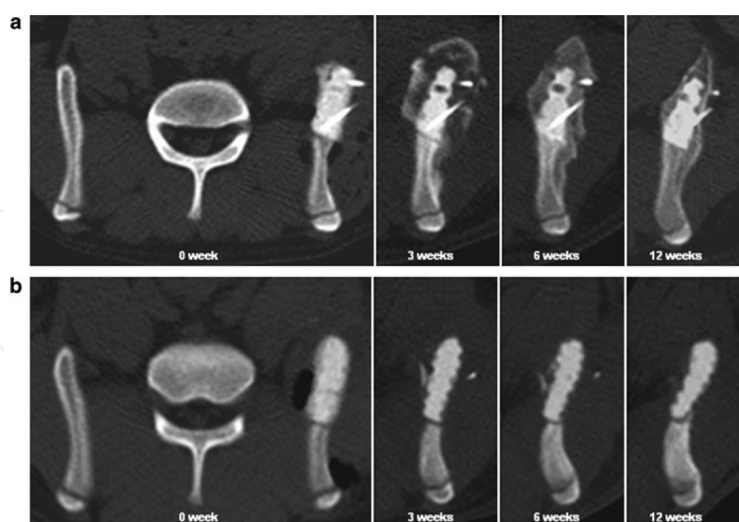


**Figure 3.** Representative mid-axial plane images of computed tomography (CT) sequentially taken over the experimental period. (a) In the BMP-treated group, radiopaque images were observed on the IP-CHA surface 3 weeks postoperatively. The radiologically dense area around the implant increased in a time-dependent manner. The implant was completely covered by new bone at 12 weeks postoperatively. (b) No significant radiopaque images were observed in the control group up to 12 weeks postoperatively.

implant fitted into the bone defect, and the IP-CHA implant prepared by CAD and CAM fitted well in all experimental and control animals. Over the 12-week study period, all animals survived without any complication.

## 3.2. Evaluation of bone defect repair using reconstructed CT images

**Figure 3** shows representative mid-axial plane images sequentially taken over the experimental period in the BMP-treated group and no-BMP control group. In the BMP-treated group, in which the IP-CHA surface was coated with the BMP-retaining dough material, radiopaque images were observed on the implant surface 3 weeks postoperatively. Thereafter, the radiologically dense area around the implant increased in a time-dependent manner, and the implant was completely covered by radiopaque images at 12 weeks postoperatively. In contrast, no significant radiopaque images were observed in the control group images up to 12 weeks postoperatively.

## 3.3. Macroscopic and histological findings

Macroscopic findings for the BMP-treated group of animals indicated that the whole implant was completely encased by a new bone, and the new bone was continuous with the original ilium, suggesting successful repair of the bone defect to the normal anatomical morphology



**Figure 4.** (a) BMP-treated group. The whole implant was completely encased by a new bone continuous with original ilium on macroscopic findings. (b) No bone tissue was observed on the implant surface in the control group.

(**Figure 4a**). In contrast, no bone tissue was observed on the implant surface in the control group of animals (**Figure 4b**). Representative histological specimens of un-decalcified tissues with Villanueva bone staining are shown (**Figure 5a–d**). In the BMP-treated group, the implant was covered by a new bone that was continuous with the original ilium, and the new bone was found to have entered pores inside the implant (**Figure 5c**). The dough material pasted on the implant surface was not observed in histological specimens obtained 12 weeks postoperatively. This indicates biodegradation during the experimental period. No inflammatory response was observed around the implant over the experimental period.
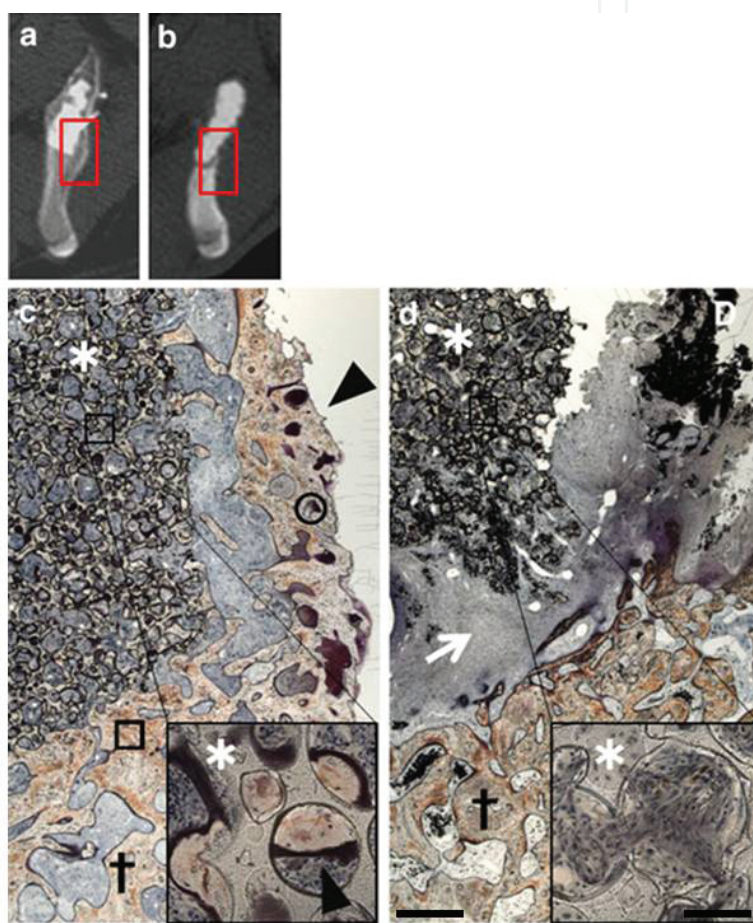


**Figure 5.** Histological sections at 12 weeks after surgery [lower (*20) and higher magnification (*200), *scale bar* indicates 100μm, 8μm in each magnification]. (a, b) Boxed area of reconstructed axial CT image shows a histological picture of (c) (BMP-treated group) and (d) (control group), respectively. (c) In the BMP-treated group, the implant was covered by a new bone that was continuous with the original ilium, and the new bone was observed in the pore of the implant. d. In the control group, no bone tissue was observed. (arrowhead: new bone, asterisk: IP-CHA implant, cross: ilium, arrow: fibrous tissue, circle: osteoid, box: calcified bone).

## 3.4. Changes over time in the amount of the new bone formed

In the BMP-treated group, the volume of the calcified new bone tissue around the implant on CT slice images of the pelvis peaked 3 weeks postoperatively, then decreased over time, and

finally resulted in the anatomical shape of the original ilium in 12 weeks postoperatively (**Figure 6**). In contrast, significant new bone formation was not observed in the control group during the observation period.
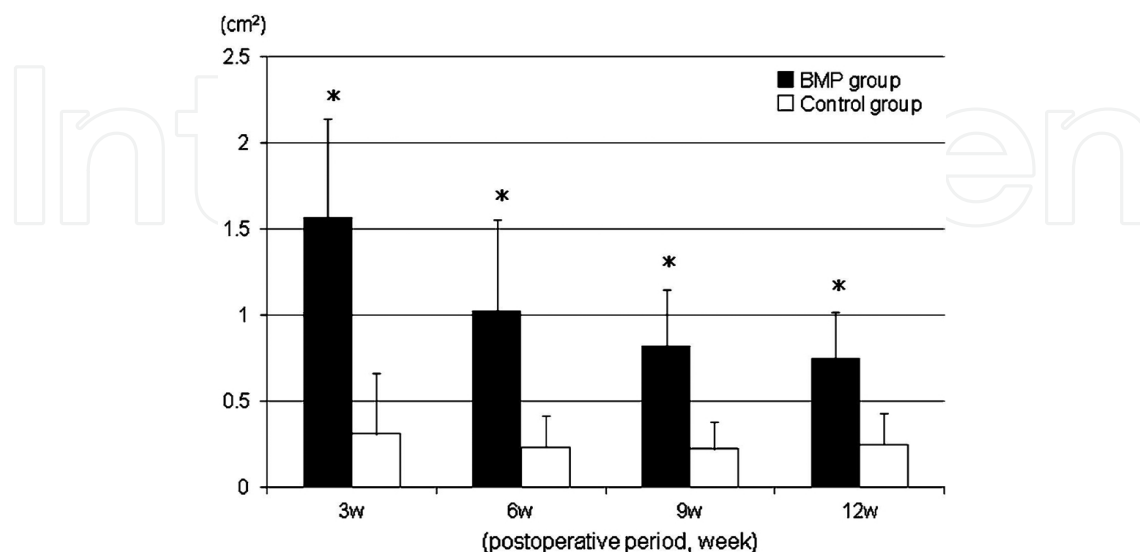


**Figure 6.** The amount of new bone formation of the BMP-treated group was significantly larger than that of the control group in reconstructed mid-axial CT planes at all experimental periods (statistical significant difference was set at $p<0.05$, values showed mean ± standard deviation).

## 4. Discussion

BMPs are established osteoinductive proteins, and BMP-2 and BMP-7, in particular, are used in combination with animal-derived collagen as a carrier for spinal fusion, pseudarthrosis treatment, and open fractures of the tibia [6–8]. These cytokine therapies accomplish a high rate of bone union and have reduced the frequency of bone grafting. However, the currently available carrier material of BMP is collagen derived from animals, which carries a possibility of infectious pathogens. We established a new DDS of BMP-2; efficacy of the rhBMP-2-retaining putty for repair of the large bone defect had been presented previously by our group in other bone defect models in beagles and posterolateral spinal fusion models in rabbits. In those experimental studies, a special A-B-A type of block copolymer (molecular weight 9,800, A;-*dl polyethylene glycol* and B; *polylactic acid)* was successfully used as the carrier material for BMP-2. The polymer was originally produced by us in collaboration with a chemical company as an optimal delivery system for rhBMP-2. Because this polymer itself was highly sticky and difficult to handle, an equal weight of biodegradable β-TCP powder was mixed with the polymer to transform it to a slightly sticky putty or dough for easy implantation. Thus far, with respect to the use of this carrier material in experimental animals, no local or systemic adverse events were noted, and no significant inflammatory reaction has been observed on histology. This synthetic carrier material is a candidate for efficacious use of rhBMP-2 to repair or reconstruct the damaged bone after extensive safety check and clinical trials. Regarding the

rhBMP-2 dose added to the implant, 100 µg of rhBMP-2 in combination with 400 mg of the delivery system (carrier material) per animal was used in the current study. This formulation was fixed based on our previous experimental results obtained in beagle models. As widely known, a minimal dose of BMP-2 to elicit local new bone formation in *in vivo* condition depends on the animal species, and humans are less sensitive to BMP-2. Therefore, a higher BMP-2 dose to the order of a few mg will be required for bone defect repair as observed in clinical reports of rhBMP-2 used for spinal body fusion, non-union of fracture, and other off-label use of rhBMP-2 in humans.

Recent reports have described successful reconstruction of maxillary bone defects in rabbits and bone union achievement in rats with pseudarthrosis using a combination of BMP gene-transfected cells and an artificial material or using sheets of cultured mesenchymal stem cells [34, 35]. However, an expensive facility equipped with a special culture system is required to establish a cell culture system for clinical application in humans. Conversely, BMPs can be conveniently used anywhere, provided that the user has adequate storage expertise. In this study, we accomplished the accurate skeletal reconstruction after resection in a virtual iliac bone tumor model in beagle dogs by combining BMP with a 3D printer, CAD, CAM, and a computer navigation system. In future, skeletal reconstruction will become possible for more specialized skeletal tissue, such as the vertebral body and load-bearing sites.

In wide resection surgery of malignant musculoskeletal tumors, optimal tumor margins and resection margin of the bone and soft tissue would be decided preoperatively on the basis of CT and/or MRI to avoid exposing the tumor tissue to the surgical field and later local recurrence of the tumor. But the accurate resection as planned preoperatively has often proven difficult. In this experimental study, a CAS system of CT-based navigation was used as a guide for bone resection margin, and the results indicated that it is possible to perform bone resection exactly as planned using the CAS system. But planning of the exact resection margin of the soft tissue covering the tumor was not attempted in this series, and similar studies based on CT and/or MRI will be necessary to determine optimal resection margin of the soft tissue.

The 3D configuration of the defect on the left iliac bone after resection of the virtual tumor was depicted on screen by subtraction of the 3D image of the left iliac bone from the 3D mirror image of the right iliac bone. CT data of the defect images were then transferred to the CAM system to drive the system to fabricate an IP-CHA implant to fill and fit the bone defect generated in the left iliac bone. The shape and size of the implants thus fabricated were acceptable and matched the defects well. However, the IP-CHA implant alone did not repair the bone defect with a new bone, as observed in control animals, in spite of its high osteoinductive capacity due to its fully interconnected porous structure. To overcome this disadvantage of the IP-CHA implant and to enhance regenerative potential of the implant, rhBMP-2 with its potent bone-inducing capacity in combination with a specific delivery system (carrier material for BMP-2) was added to the surface of the IP-CHA implant. This successfully elicited new bone formation on the surface of the implant and restored normal anatomical surface contour of the iliac bone in 12 weeks using the IP-CHA non-degradable block within the new bone mass. Replacement of the non-biodegradable IP-CHA block by a porous β-TCP implant might have resulted in complete regeneration of the bone defect without remnant biomaterials.

However, because of the highly fragile nature of the porous TCP and easy breakage of the implant during fabricating and surgical procedures, the IP-CHA implant was used in this study, and the bone mass with stable connection to the original iliac bone and porous implant was created.

Recent developments in 3D printing have expanded its range of application to include production of implants, scaffolds for tissue engineering, and instruments for DDSs in addition to visualization of surgical sites preoperatively and casting of surgical tools on the basis of the additive manufacturing technology used in the present study. In addition, it has become possible to directly print biological materials onto solvent-free, aqueous-based 3D scaffolds for tissue transplantation [36–38]. Using CAD/CAM techniques, spatially defined implants can be constructed by attaching functional living cells, physiological substances, and bioactive factors in layers to organ scaffolds created on the basis of MRI or CT. For this bioprinting technique, three major modes are currently available: inkjet, micro-extrusion, and laser-assisted bioprinting. These modes differ in various properties, such as the range of material viscosity accommodated, gelling method, viability, and concentration of cells to be handled. Skin and cartilage regeneration by the inkjet method, creating heart valves and blood vessels by the micro-extrusion method, and creating skin containing the heart tissue or cells by the laser-assisted method have been reported [37, 38]. We expect that for cases involving extensive tissue defects or requiring organ transplantation, printing technologies, scaffold development, cell surgical techniques, and the use of growth factors will advance further and the scope of clinical application will be further broadened if necessary tissues can be created in a shorter period of time in the future.

# 5. Conclusion

Advances in computer-assisted techniques have led to computer-assisted preoperative planning, custom production of surgical implants using patient data, and use of navigation systems in orthopedics. In this study, we accomplished accurate skeletal reconstruction after resection in a virtual iliac bone tumor model in beagle dogs by combining BMP with a 3D printer, CAD, CAM, and a computer navigation system. In future, skeletal reconstruction will become possible for more specialized skeletal tissues, such as the vertebral body and load-bearing sites. Moreover, in future, the development of bioprinting techniques may enable us to reconstruct extensive tissue defects or organ transplantation.

# Author details

Koichi Yano[1*], Takashi Namikawa[2], Takuya  Uemura[3], Yasunori Kaneshiro[1] and
Kunio Takaoka[4]

*Address all correspondence to: koichiyano@hotmail.com

1 Department of Orthopaedic Surgery, Seikeikai Hospital, Sakai city, Japan

2 Department of Orthopaedic Surgery, Osaka City General Hospital, Osaka city, Japan

3 Department of Orthopaedic Surgery, Osaka City University Graduate School of Medicine, Osaka city, Japan

4 Department of Orthopaedic Surgery, Nishinomiya Watanabe Hospital, Nishinomiya city, Japan

## References

[1] Buck BE, Malinin TI. Human bone and tissue allografts. Preparation and safety. Clin Orthop Relat Res. 1994;Jun(303):8–17.

[2] Arrington ED, Smith WJ, Chambers HG, Bucknell AL, Davino NA. Complications of iliac crest bone graft harvesting. Clin Orthop Relat Res. 1996;Aug(329):300–9.

[3] Butler D. Last chance to stop and think on risks of xenotransplants. Nature. 1998;22(391):320–4.

[4] DeLustro F, Dasch J, Keefe J, Ellingsworth L. Immune responses to allogeneic and xenogeneic implants of collagen and collagen derivatives. Clin Orthop Relat Res. 1990;Nov(260):263–79.

[5] Oryan A, Alidadi S, Moshiri A, Maffulli N. Bone regenerative medicine: classic options, novel strategies, and future directions. J Orthop Surg Res. 2014;17(9):24628910. DOI: 10.1186/1749-799X-9-18

[6] Boden SD, Kang J, Sandhu H, Heller JG. Use of recombinant human bone morphogenetic protein-2 to achieve posterolateral lumbar spine fusion in humans: a prospective, randomized clinical pilot trial: 2002 Volvo Award in clinical studies. Spine (Phila Pa 1976). 2002;27(23):2662–73.

[7] Burkus JK, Transfeldt EE, Kitchel SH, Watkins RG, Balderston RA. Clinical and radiographic outcomes of anterior lumbar interbody fusion using recombinant human bone morphogenetic protein-2. Spine (Phila Pa 1976). 2002;27(21):2396–408.

[8] Friedlaender GE, Perry CR, Cole JD, Cook SD, Cierny G, Muschler GF, Zych GA, Calhoun JH, LaForte AJ, Yin S. Osteogenic protein-1 (bone morphogenetic protein-7) in the treatment of tibial nonunions. J Bone Joint Surg Am. 2001;83(Suppl 1):S151–8.

[9] Brown GA, Milner B, Firoozbakhsh K. Application of computer-generated stereolithography and interpositioning template in acetabular fractures: a report of eight cases. J Orthop Trauma. 2002;16(5):347–52.

[10] Takeyasu Y, Oka K, Miyake J, Kataoka T, Moritomo H, Murase T. Preoperative, computer simulation-based, three-dimensional corrective osteotomy for cubitus varus

deformity with use of a custom-designed surgical device. J Bone Joint Surg Am. 2013;95(22):e173. DOI: 10.2106/JBJS.L.01622

[11] Bellemans J, Vandenneucker H, Vanlauwe J. Robot-assisted total knee arthroplasty. Clin Orthop Relat Res. 2007;Nov(464):111–6.

[12] Fujishiro T, Nakaya Y, Fukumoto S, Adachi S, Nakano A, Fujiwara K, Baba I, Neo M. Accuracy of pedicle screw placement with robotic guidance system: a cadaveric study. Spine (Phila Pa 1976). 2015;40(24):1882–9. DOI: 10.1097/BRS.0000000000001099

[13] Ieguchi M, Hoshi M, Takada J, Hidaka N, Nakamura H. Navigation-assisted surgery for bone and soft tissue tumors with bony extension. Clin Orthop Relat Res. 2012;470(1): 275–83. DOI: 10.1007/s11999-011-2094-5

[14] Yoshikawa H, Tamai N, Murase T, Myoui A. Interconnected porous hydroxyapatite ceramics for bone tissue engineering. J R Soc Interface. 2009;6(Suppl 3):S341–8. DOI: 10.1098/rsif.2008.0425

[15] Saito N, Okada T, Horiuchi H, Murakami N, Takahashi J, Nawata M, Ota H, Nozaki K, Takaoka K. A biodegradable polymer as a cytokine delivery system for inducing bone formation. Nat Biotechnol. 2001;19(4):332–5.

[16] Miyamoto S, Takaoka K, Okada T, Yoshikawa H, Hashimoto J, Suzuki S, Ono K. Polylactic acid-polyethylene glycol block copolymer. A new biodegradable synthetic carrier for bone morphogenetic protein. Clin Orthop Relat Res. 1993;Sep(294):333–43.

[17] Saito N, Okada T, Toba S, Miyamoto S, Takaoka K. New synthetic absorbable polymers as BMP carriers: plastic properties of poly-D,L-lactic acid-polyethylene glycol block copolymers. J Biomed Mater Res. 1999;47(1):104–10.

[18] Saito N, Okada T, Horiuchi H, Murakami N, Takahashi J, Nawata M, Ota H, Miyamoto S, Nozaki K, Takaoka K. Biodegradable poly-D,L-lactic acid-polyethylene glycol block copolymers as a BMP delivery system for inducing bone. J Bone Joint Surg Am. 2001;83-A Suppl 1(Pt 2):S92–8.

[19] Murakami N, Saito N, Horiuchi H, Okada T, Nozaki K, Takaoka K. Repair of segmental defects in rabbit humeri with titanium fiber mesh cylinders containing recombinant human bone morphogenetic protein-2 (rhBMP-2) and a synthetic polymer. J Biomed Mater Res. 2002;62(2):169–74.

[20] Murakami N, Saito N, Takahashi J, Ota H, Horiuchi H, Nawata M, Okada T, Nozaki K, Takaoka K. Repair of a proximal femoral bone defect in dogs using a porous surfaced prosthesis in combination with recombinant BMP-2 and a synthetic polymer carrier. Biomaterials. 2003;24(13):2153–9.

[21] Saito N, Okada T, Horiuchi H, Ota H, Takahashi J, Murakami N, Nawata M, Kojima S, Nozaki K, Takaoka K. Local bone formation by injection of recombinant human bone morphogenetic protein-2 contained in polymer carriers. Bone. 2003;32(4):381–6.

[22] Yoneda M, Terai H, Imai Y, Okada T, Nozaki K, Inoue H, Miyamoto S, Takaoka K. Repair of an intercalated long bone defect with a synthetic biodegradable bone-inducing implant. Biomaterials. 2005;26(25):5145–52.

[23] Kato M, Toyoda H, Namikawa T, Hoshino M, Terai H, Miyamoto S, Takaoka K. Optimized use of a biodegradable polymer as a carrier material for the local delivery of recombinant human bone morphogenetic protein-2 (rhBMP-2). Biomaterials. 2006;27(9):2035–41.

[24] Suzuki A, Terai H, Toyoda H, Namikawa T, Yokota Y, Tsunoda T, Takaoka K. A biodegradable delivery system for antibiotics and recombinant human bone morphogenetic protein-2: a potential treatment for infected bone defect. J Orthop R. 2003;24(3): 327–32.

[25] Saito N, Murakami N, Takahashi J, Horiuchi H, Ota H, Kato H, Okada T, Nozaki K, Takaoka K. Synthetic biodegradable polymers as drug delivery systems for bone morphogenetic proteins. Adv Drug Deliv Rev. 2005;57(7):1037–48.

[26] Kato M, Namikawa T, Terai H, Hoshino M, Miyamoto S, Takaoka K. Ectopic bone formation in mice associated with a lactic acid/dioxanone/ethylene glycol copolymer-tricalcium phosphate composite with added recombinant human bone morphogenetic protein-2. Biomaterials. 2006;27(21):3927–33.

[27] Namikawa T, Terai H, Suzuki E, Hoshino M, Toyoda H, Nakamura H, Miyamoto S, Takahashi N, Ninomiya T, Takaoka K. Experimental spinal fusion with recombinant human bone morphogenetic protein-2 delivered by a synthetic polymer and beta-tricalcium phosphate in a rabbit model. Spine (Phila Pa 1976). 2005;30(15):1717–22.

[28] Hoshino M, Egi T, Terai H, Namikawa T, Takaoka K. Repair of long intercalated rib defects using porous beta-tricalcium phosphate cylinders containing recombinant human bone morphogenetic protein-2 in dogs. Biomaterials. 2006;27(28):4934–40.

[29] Hoshino M, Namikawa T, Kato M, Terai H, Taguchi S, Takaoka K. Repair of bone defects in revision hip arthroplasty by implantation of a new bone-inducing material comprised of recombinant human BMP-2, Beta-TCP powder, and a biodegradable polymer: an experimental study in dog. J Orthop R. 2007;25(8):1042–51.

[30] Taguchi S, Namikawa T, Ieguchi M, Takaoka K. Reconstruction of bone defects using rhBMP-2-coated devitalized bone. Clin Orthop Relat Res. 2007;Aug(461):162–9.

[31] Tokuhara Y, Wakitani S, Imai Y, Kawaguchi A, Fukunaga K, Kim M, Kadoya Y, Takaoka K. Repair of experimentally induced large osteochondral defects in rabbit knee with various concentrations of Escherichia coli-derived recombinant human bone morphogenetic protein-2. Int Orthop. 2010;34(5):761–7.

[32] Hoshino M, Egi T, Terai H, Namikawa T, Kato M, Hashimoto Y, Takaoka K. Repair of long intercalated rib defects in dogs using recombinant human bone morphogenetic

protein-2 delivered by a synthetic polymer and beta-tricalcium phosphate. J Biomed Mater Res A. 2009;90(2):514–21.

[33] Yano K, Hoshino M, Ohta Y, Manaka T, Naka Y, Imai Y, Sebald W, Takaoka K. Osteoinductive capacity and heat stability of recombinant human bone morphogenetic protein-2 produced by *Escherichia coli* and dimerized by biochemical processing. J Bone Miner Metab. 2009;27(3):355–63. DOI: 10.1007/s00774-009-0040-3

[34] Li J, Li Y, Ma S, Gao Y, Zuo Y, Hu J. Enhancement of bone formation by BMP-7 transduced MSCs on biomimetic nano-hydroxyapatite/polyamide composite scaffolds in repair of mandibular defects. J Biomed Mater Res A. 2010;95(4):973–81. DOI: 10.1002/jbm.a.32926

[35] Nakamura A, Akahane M, Shigematsu H, Tadokoro M, Morita Y, Ohgushi H, Dohi Y, Imamura T, Tanaka Y. Cell sheet transplantation of cultured mesenchymal stem cells enhances bone formation in a rat nonunion model. Bone. 2010;46(2):418–24. DOI: 10.1016/j.bone.2009.08.048

[36] Do AV, Khorsand B, Geary SM, Salem AK. 3D printing of scaffolds for tissue regeneration applications. Adv Healthc Mater. 2015;4(12):1742–62. DOI: 10.1002/adhm.201500168

[37] Chia HN, Wu BM. Recent advances in 3D printing of biomaterials. J Biol Eng. 2015;9(4): 25866560. DOI: 10.1186/s13036-015-0001-4

[38] Murphy SV, Atala A. 3D bioprinting of tissues and organs. Nat Biotechnol. 2014;32(8): 773–85. DOI: 10.1038/nbt.2958